Am J Transl Res 2020;12(11):7127-7143
www.ajtr.org /ISSN:1943-8141/AJTR0109786

Original Article

Selaginellin B induces apoptosis and autophagy in pancreatic cancer cells via the JAK2/STAT3 signaling pathway

Peng Chu[1,2*], Shisheng Wang[3*], Xinxing Zhu[2*], Ying Yang[4], Hailong Li[2], Tsehaye Tesfaldet[2], Abdullah Shopit[2], Yongliang Yang[3], Xiaodong Ma[2], Jinyong Peng[2], Zeyao Tang[2], Zhaolin Sun[1,2]

[1]Department of Biochemistry and Molecular Biology, [2]Basic and Applied Research on Pharmacodynamic Substances of Traditional Chinese Medicine of Liaoning Province, Dalian Medical University, Dalian, China; [3]School of Chemical Engineering, Dalian University of Technology, Dalian, China; [4]The Second Affiliated Hospital, Neurological Intensive Care Unit, Dalian Medical University, Dalian, China. [*]Equal contributors.

Received November 28, 2019; Accepted June 4, 2020; Epub November 15, 2020; Published November 30, 2020

Abstract: Selaginella tamariscina (ST), a well-known traditional medicinal plant, has been used to treat various cancers, including pancreatic cancer. However, the underlying mechanism by which Selaginellin B, a natural pigment isolated and purified from ST, protects against pancreatic cells has yet to be fully elucidated. In the present study, the biological functions of Selaginellin B were investigated using apoptosis, migration and colony formation assays in ASPC-1 and PANC-1 cells. In addition, apoptosis-associated proteins were detected by Western blotting. Our results demonstrated that Selaginellin B induced apoptosis, as evidenced by the increased cleaved caspase-3 level and Bax/Bcl-2 ratio. Moreover, Selaginellin B led to a marked up-regulation of the ratio of LC3-II/LC3-I in ASPC-1 and PANC-1 cells, respectively. Furthermore, reverse pharmacophore screening, molecular docking and molecular dynamics simulation studies revealed that Janus kinase 2 (JAK2) may be a potential target for Selaginellin B. In summary, the results of the present research have demonstrated that Selaginellin B is an effective anticancer agent against PANC-1 and ASPC-1 cells, and the compound holds great promise for the treatment of pancreatic cancer.

Keywords: Selaginellin B, reverse pharmacophore screening, pancreatic cancer cell, apoptosis

Introduction

Pancreatic cancer (PC), a fatal solid malignancy with poor prognosis, exerts a significant public health burden globally. It is the fourth leading cause of mortality among all cancer cases in the United States [1-3], and is the sixth primary reason of cancer-associated mortality, with a 5-year survival rate of 1-3% in China [4, 5]. Currently, chemotherapy is of utmost importance therapy for patients with metastatic PC. Compared with gemcitabine, certain chemotherapeutic drugs, such as 5-fluorouracil, leucovorin and oxaliplatin, have achieved survival benefits for PC patients. However, serious adverse side-effects and the problem of multidrug resistance limit their clinical applicability [6, 7]. Therefore, developing novel drugs with high efficiency and minimal adverse effects are urgently needed.

Selaginella tamariscina (Beauv.) (ST), one of the traditional Chinese herbal medicines, has been used in the treatment of cancer, hepatitis, cardiovascular diseases, and trauma [8, 9]. Selaginellin has a unique structure owing to the presence of a pigment-like scaffold [10]. In many pharmacological studies, Selaginellin and its 15 derivatives (selaginellin A-N) have shown strong biological activity, including their inhibitory effects on the proliferation of HeLa cells, as well as their protective effects against cytotoxicity in differentiated PC12 cells [10, 11]. However, the anti-PC effects of ST on cellular proliferation and the underlying mechanism(s) remain unclear.

In recent years, target fishing has emerged as a very useful technique in the campaign for the discovery of small molecular compounds with biological activities. The underlying idea of this

technique is to integrate biological information with chemical databases and then predict the biological activity of compounds through their structures. It is anticipated that computational target fishing technologies will have a profound impact on drug development and these have made target recognition more accurate and efficient [12, 13]. To date, new computational target identification methods are springing up vigorously, including reverse pharmacophore screening, molecular docking studies, and molecular dynamics (MD) simulation [13]. In the current study, these methodologies have been utilized in an attempt to identify the potential protein targets of the isolated compounds in order to further delineate the anticancer effects of selaginellin B.

Janus kinases (JAKS; namely, JAK1, JAK2, JAK3 and Tyk2) play a key role in modulating multiple signaling pathways that dominate cellular survival, differentiation, proliferation, immigration and apoptosis. JAKs/STAT signaling has been demonstrated to play a significant role in oncogenesis and development of PC [14, 15]. The mRNA levels of JAK2 and STAT3 were shown to be overexpressed in clinical PC samples. In addition, monitoring the protein levels of JAK2 and STAT3 was reported to be of clinical importance in PC tissues [15, 16]. Taken together, suppression of the JAK2/STAT3 signalling pathway has been shown to be a promising therapeutic target in PC prevention and treatment.

Therefore, the aim of this study was to investigate the anti-tumor activities of Selaginellin B on human PC cells in vitro in order to elucidate the potential mechanisms. The findings may provide novel insights into the development of potential therapeutic candidates for preventing PC.

Material and methods

Materials

Standard commercial solvents and reagents were directly used without further purifications. Silica gel was purchased from Qingdao Haiyang Chemical Co. Ltd, ESI-MS was performed on a LC-Q-TOF/MS system, ^{1}H-NMR spectra were performed on Bruker DRX-400 with TMS as a reference. The primary antibodies against JAK2, phosphorylated (p)-JAK2, STAT3, p-STAT3, cleaved caspase-3, Bax, Bcl-2 and β-actin were purchased from Proteintech Group, Inc. (Chicago, IL, USA), whereas all the secondary antibodies were obtained from Abbkine Scientific Co., Ltd. (Redlands, California, USA). The Apoptosis and Cell Cycle Analysis Kit were obtained from Beyotime Institute of Biotechnology (Haimen, Jiangsu, China). All other chemicals were purchased from Sigma Chemical Co. (now a brand of Merck KGaA). Normal pancreatic ductal epithelial cells (the HPDE6-C7 cell line), and the human PC cell lines (ASPC-1 and PANC-1), were obtained from the Shanghai Institute of Biochemistry and Cell Biology (Shanghai, China).

Separation and identification of Selaginellin B

Dried powder of Selaginella tamariscina (1 kg) was reflux extracted with 95% EtOH as solvent (volume ratio of 1:5). The EtOH extract was concentrated and partitioned with petroleum ether and ethyl acetate. The ethyl acetate fraction (16.1 g) was separated by a combination of chromatographies such as silica gel column chromatography, preparative thin-layer chromatography, and preparative high performance liquid chromatography to yield 11 compounds including Selaginellin B (6.7 mg).

Selaginellin B, red powder; ESI-MS *m/z* 495.25 $[M + H]^-$; ^{1}HMR (400 MHz, acetone-d6): δ 6.52 (4H, d, J = 9.2 Hz), 7.13 (4H, d, J = 9.2 Hz), 7.45 (1H, d, J = 8.0 Hz), 7.23 (1H, d, J = 8.0 Hz), 6.85 (2H, d, J = 8.4 Hz), 6.63 (2H, d, J = 8.4 Hz), 7.09 (2H, d, J = 8.6 Hz), 6.73 (2H, d, J = 8.6 Hz), 2.61 (3H, s). This is consistent with the characteristics of Selaginellin B [10]. Selaginellin B was dissolved with 0.1% dimethylsulfoxide and stored at 20°C for in vitro experiments.

Cell culture

The ASPC-1, HPDE6-C7, and PANC-1 cells were cultured in high-glucose DMEM supplemented with 10% fetal bovine serum (FBS), 1% penicillin and streptomycin mixture, and maintained in an atmosphere of 5% CO_2 at 37°C under conditions of saturated humidity.

Cell viability assay

The human PC cells were inoculated into 96 well plates at a density of 6×10^3 cells/well and incubated overnight to allow adherence to

occur. They were subsequently treated with Selaginellin B at different concentrations (1, 5, 10 and 20 μM). Cell growth was detected at 12 h, 24 h and 48 h respectively. Each well was subsequently treated with 15 μl MTT solution (final concentration: 5 mg/ml). After incubated the reaction at 37°C for 4 h, the formazan crystals were dissolved in DMSO, then add 20 μl DMSO to each well to dissolve formazan crystals and measure the absorbance values at 490 nm by a microplate reader (Multiskan MK3; Shaanxi Pioneer Biotech Co., Ltd., Xi'an, China). Cell viability (%) was calculated using the average absorbance of different treatment groups/average absorbance of control groups × 100%. Experiments were conducted in triplicates.

Apoptosis assay

Apoptosis was measured using a FITC Annexin V apoptosis detection kit. Incubation of cells with different doses of Selaginellin B for 24 h. The cells were collected cells and washed twice with cold PBS, then were resuspend in 1 × Binding Buffer at a concentration of 1×10^6 cells/ml. subsequently, the cells were dyed simultaneously with FITC Annexin V and PI for 15 min at room temperature in the dark. Flow cytometry was performed with a BD FACSAria™ II flow cytometer (BD Biosciences, San Jose, CA, USA) to count 10000 cells for each experiment. Flow cytometry data were finally analyzed using FlowJo version 7.6.1 (FlowJo, LLC, USA). Each experiment was carried out in triplicate.

In vitro migration assay

Cell migration was observed using a scratch wound (wound-healing) assay. The cells (5×10^5 cells/well) were seeded into 6-well plates, cultured in an atmosphere of 5% CO_2 at 37°C under conditions of saturated humidity overnight, and subsequently scraped a line by a 200 μl aseptic pipette tip. Cells were treated with the doses of Selaginellin B indicated above in medium without FBS. After incubation for a further 24 h, cells were washed with PBS for 3 times, and images of the cells were obtained using a microscope (Nikon, Japan). The wound healing rate was calculated using the following formula: (average wound margin in 0 h - average wound margin in 24 h)/average wound margin in 0 h. Experiments were conducted in triplicates.

Colony formation assay

In order to verify sensitivity of the cells to Selaginellin B, a colony formation assay *in vitro* was used. Briefly, cells (1,000 cells/well) plated in 6 well plates were treated with different doses of Selaginellin B (0, 5, 10 μM). After incubation at 37°C for 24 h, the cells were subsequently washed with PBS after 12 h, then replenish fresh medium containing 10% fetal bovine serum. After 14 days of incubation in an atmosphere of 5% CO_2 at 37°C, the colonies were photographed using the camcera (SONYDSC-W800) after staining with 0.1% crystal violet. Clones containing > 50 cells were counted for statistical analysis. Three independent assays were performed.

Cell cycle analysis

According to the instructions of cell cycle analysis kit. 5×10^5 cells were seeded into 6-well plates, incubated with Selaginellin B. After 24 hours of treatment, the cells were collected following centrifugation and added 1 ml of ice bath precooled 70% ethanol and fix at 4°C for 2 hours or longer. The samples were then suspended with PI staining reagent (50 μg/ml PI and 1 mg/ml RNAse in 1 ml of sodium citrate buffer) at 37°C for 30 min. Finally, Flow cytometry was used to detect red fluorescence and light scattering at 488 nm. The data were finally analyzed using FlowJo version 7.6.1 (FlowJo, LLC, USA).

Transmission electron microscopy (TEM)

The human PC cells were plated in 6-well plates, treated with 0 and 5 μM Selaginellin B, and cultured at 37°C for 24 h. Cells were collected and fixed overnight in 0.1 M PBS at 4°C with 2% glutaraldehyde. The samples were subsequently dehydrated, embedded, sectioned. Uranium acetate and lead citrate were double dyed. Electron micrographs were recorded using a transmission electron microscope (JEM-2000EX; JEOL Ltd., Tokyo, Japan).

Targets predicted by PharmMapper

PharmMapper, an open-source online platform (http://www.lilab-ecust.cn/pharmmap per) for

pharmacophore matching and potential target identification, was used for the prediction of molecular targets. The molecular file of Selaginellin B was uploaded to the PharmMapper servers for *in silico* screening. The number of matched potential targets was set to 300, whereas remaining settings were considered as default.

Molecular modeling

The PDB file of Selaginellin B were generated using the PRODRG Server [17], and the protein structures were obtained from the RCSB Protein Data Bank. The protein structures were cleaned by removing crystallographic water, and prepared by the addition of polar hydrogen atoms, followed by the addition of Gasteiger charges. AutoDock 4.2 with MGL tools 1.5.6 were applied to molecular docking analysis [18], and residual interactions at the protein-drug interface were evaluated using LigPlot [19].

MD simulation

The conformations of the complexes formed between Selaginellin B and the potential target protein were predicted using the AutoDock 4.2 program, and each MD simulation was performed by Gromacs 5.1.5 in the Amber99sb force field. On the basis of molecular dynamics simulation, the binding free energy of Selaginellin B with potential target proteins was calculated by molecular mechanics energy binding Poisson Boltzmann specific surface area (MM/PBSA) methods.

Western blot analysis

Following the separation of the sample proteins by gel electrophoresis, The proteins were subsequently transferred to PVDF membranes and the membranes were incubated in a closed buffer (5% skimmed milk) at 25°C for 2 hours. Western blots were probed with the primary antibodies (1:1,000 dilution) at 4°C overnight. Then washing with TBST, the membranes were incubated with HRP conjugated secondary antibody (1:2,000 dilution) at 37°C for 1 h. The blots were then detected using enhanced chemiluminescence reagent (Thermo Fisher Scientific, Inc.), and photographs were captured using the Bio Spectrum Gel Imaging system (UVP LLC, Upland, CA, USA).

Statistical analysis

Statistical differences between groups were assessed using a One-way analysis of variance (ANOVA). Results are expressed as the mean ± SD. Two groups were compared with a two-tailed Student's t-test using Graph Pad Prism 5 (Graph Pad Software, Inc., San Diego, CA, USA). Bonferroni's test was used to correct multiple comparisons, and P values <0.05 were considered statistically significant.

Results

Structural elucidation

Selaginellin B was obtained as a red powder, with the molecular formula $C_{34}H_{24}O_4$, deduced from ESI-MS on the basis of the quasi-molecular ion peak at m/z 495.25 $[M + H]^-$. The ^1H NMR data of Selaginellin B were consistent with previous studies (**Figures 1A** and S1) [10].

Effect of Selaginellin B on cell viability and morphology of PC cells

To identify the cytotoxic effect of Selaginellin B in HPDE6-C7 and ASPC-1 and PANC-1 cells, the cells were treated with different concentrations of Selaginellin B for subsequent analysis using MTT assay (**Figure 1C-E**). The concentration of the drug that led to 50% inhibition (i.e., the IC_{50} value) following 24 h of Selaginellin B treatment was determined to be 6.4 μM in the ASPC-1 cells, and 8.8 μM for the PANC-1 cells. In addition, the results demonstrated that Selaginellin B suspended the cell viability of the ASPC-1 and PANC-1 cell lines in both concentration- and time-dependent manner. However, Selaginellin B showed less toxicity towards HPDE6-C7 cells, suggesting that Selaginellin B may be a promising anti-PC agent. Furthermore, treatment with Selaginellin B led to marked cellular morphological changes, including rounding and blebbing of the cells, and a reduction in cell-to-cell interactions, as shown in **Figure 1B**.

Selaginellin B induces apoptosis in the pancreatic cancer cells

To examine whether the antitumor activity of Selaginellin B was associated with apoptosis in PC, Annexin V-FITC and PI double staining was performed using flow cytometry analysis. Marked increases in the apoptotic rates were

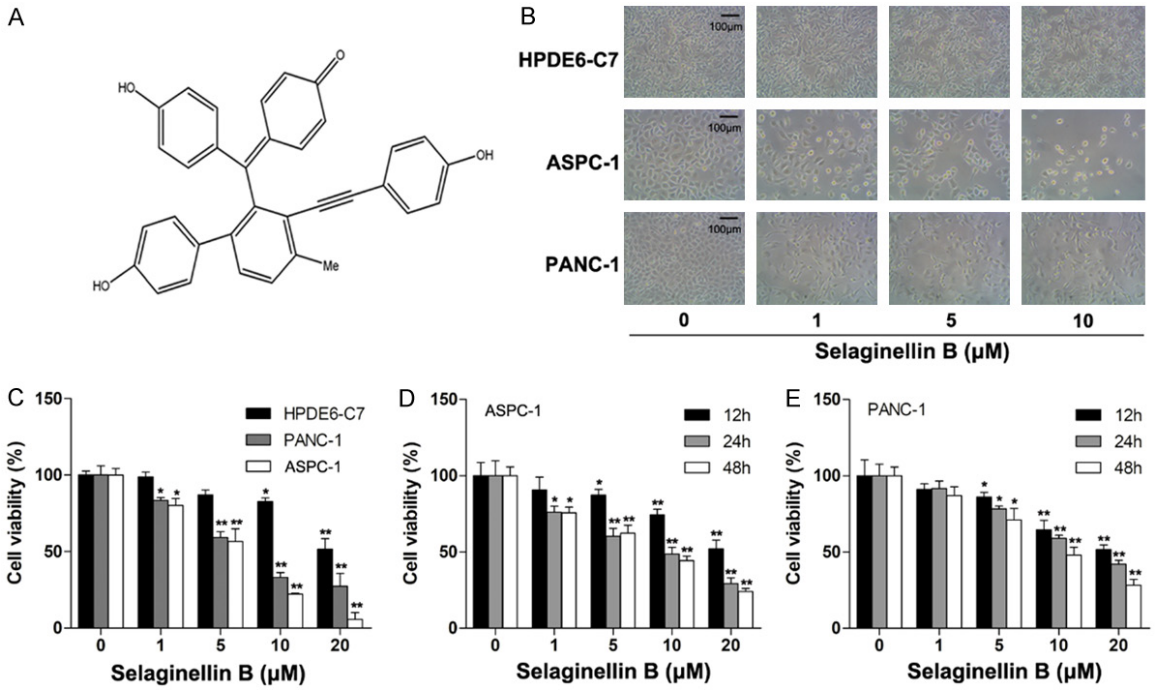

Figure 1. Selaginellin B changed the morphology and inhibited the cell viability. A. The chemical structures of Selaginellin B. B. The morphological changes of HPDE6-C7, ASPC-1, and PANC-1 cells treated with Selaginellin B (1, 5 and 10 μM) for 24 h. Scale bar = 100 μm. C. Inhibitory effect of Selaginellin B on the ASPC-1, PANC-1 and HPDE6-C7 cell lines. Cells were treated with Selaginellin B at concentrations ranging from 1-20 μM, and cell viability was measured by the MTT assay after treatment for 24 h. D, E. Inhibitory effect of Selaginellin B on the ASPC-1 and PANC-1 cell lines. Cells were treated with Selaginellin B at concentrations ranging from 1-20 μM, and cell viability was measured by the MTT assay after treatment for 12, 24 and 48 h. Values are expressed as the mean ± SD of 3 independent experiments. $^{*}P<0.05$; $^{**}P<0.01$ vs. the control group.

observed, from 6.69% (in the control group) to 12.01, 22.90, and 41.70% in the ASPC-1 cells, and from 2.69% (control group) to 8.46, 17.07, and 24.05% in the PANC-1 cells, upon treatment for 24 h with 1, 5 and 10 μM Selaginellin B, respectively (**Figure 2A**). The levels of apoptosis-associated proteins were subsequently investigated by Western blot analysis. The ratio of Bax/Bcl-2, which regulates apoptosis by regulating mitochondrial membrane permeability [16], was increased by Selaginellin B. The levels of procaspase-9 and procaspase-3 were shown to be inhibited, whereas that of cleaved caspase-3 was increased, by Selaginellin B (**Figure 2B**). These results suggested that Selaginellin B could induce apoptosis in ASPC-1 and PANC-1 cells in a concentration-dependent manner.

Effect of Selaginellin B on cell cycle distribution of ASPC-1 and PANC-1 cells

To explore the cancer cell growth inhibitory mechanisms of Selaginellin B, subsequently, the effect of Selaginellin B on cell cycle arrest in PC cells was examined. The results showed that Selaginellin B treatment caused an accumulation of the two PC cell lines in the G1-phase. As shown in **Figure 3**, the percentages of ASPC-1 and PANC-1 cells in the G1-phase were increased from 42.88% in the control treament group to 55.91% in the 10 μM Selaginellin B group for the ASPC-1 cells, and from 53.41% in the control treatment group to 69.67% in the 10 μM Selaginellin B group for the PANC-1 cells. These findings suggested that Selaginellin B could induce G1-phase arrest of the PC cells.

Suppression of the migration and colony formation of PC cells by Selaginellin B

As shown in **Figure 4A** after 24 h of incubation, for the control groups of the migrating cells (ASPC-1 and PANC-1 cell lines), the wound between cell layers formed after the scratch was made was almost entirely occupied by cells, whereas for the groups that were treated with Selaginellin B, the cells were prevent-

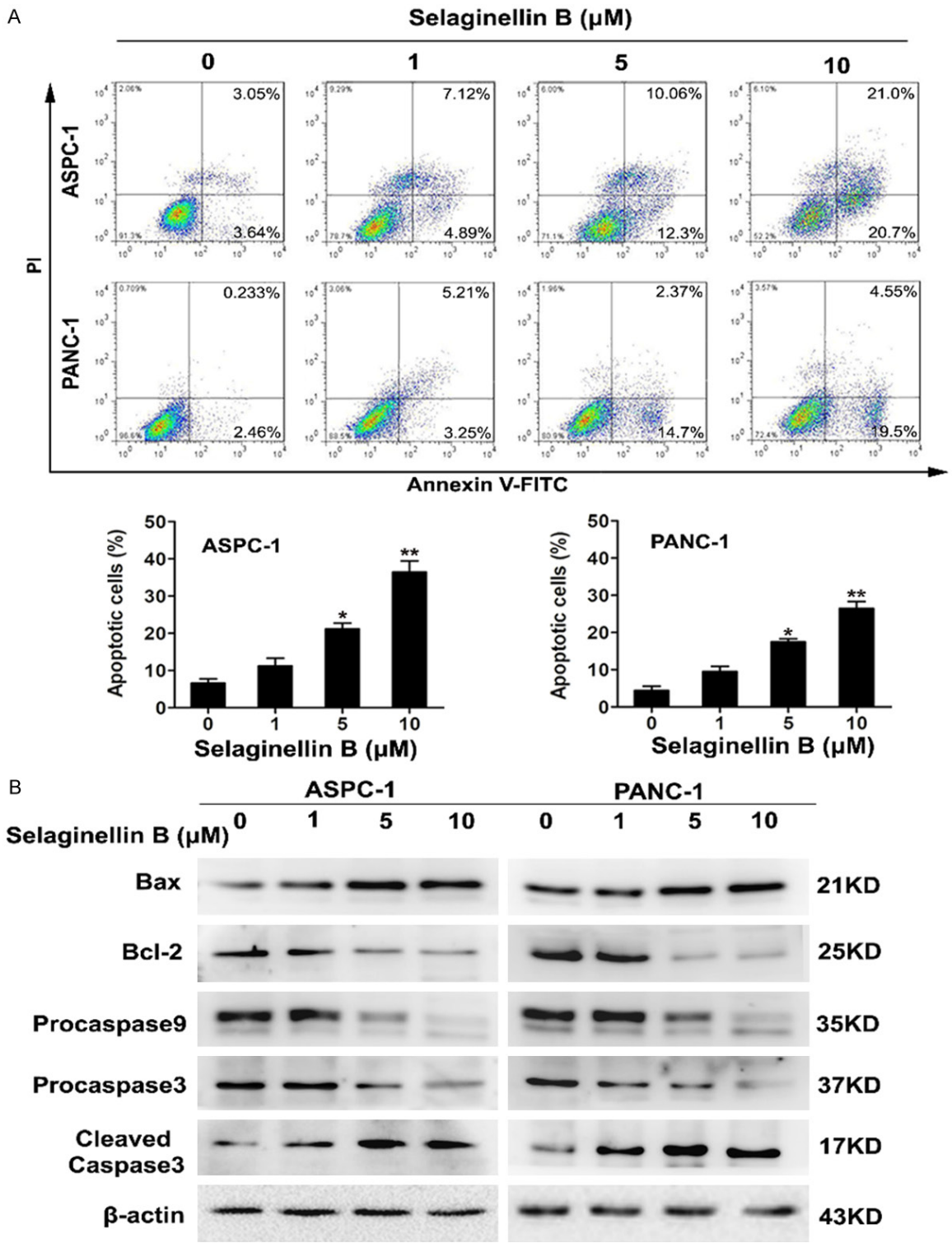

Figure 2. Apoptosis induction of Selaginellin B in the pancreatic cancer cells. A. Flow cytometric analysis of the apoptosis induction of Selaginellin B in the ASPC-1 and PANC-1 cells. After treatment with Selaginellin B at concentrations of 1, 5 and 10 μM for 24 h, the cells were stained with annexin V-FITC and PI, and subsequently analyzed by flow cytometry. The dot plots have been obtained from 1 out of 3 independent experiments, performed in the same experimental conditions, which gave similar results. The values are expressed as the mean ± SD of 3 independent experiments. $^{*}P<0.05$; $^{**}P<0.01$ vs. the control group. B. Western blot analysis was performed to determine the apoptosis pathway induced by Selaginellin B in the ASPC-1 and PANC-1 cells. Cells were treated with different concentrations of Selaginellin B (1, 5 and 10 μM) for 24 h.

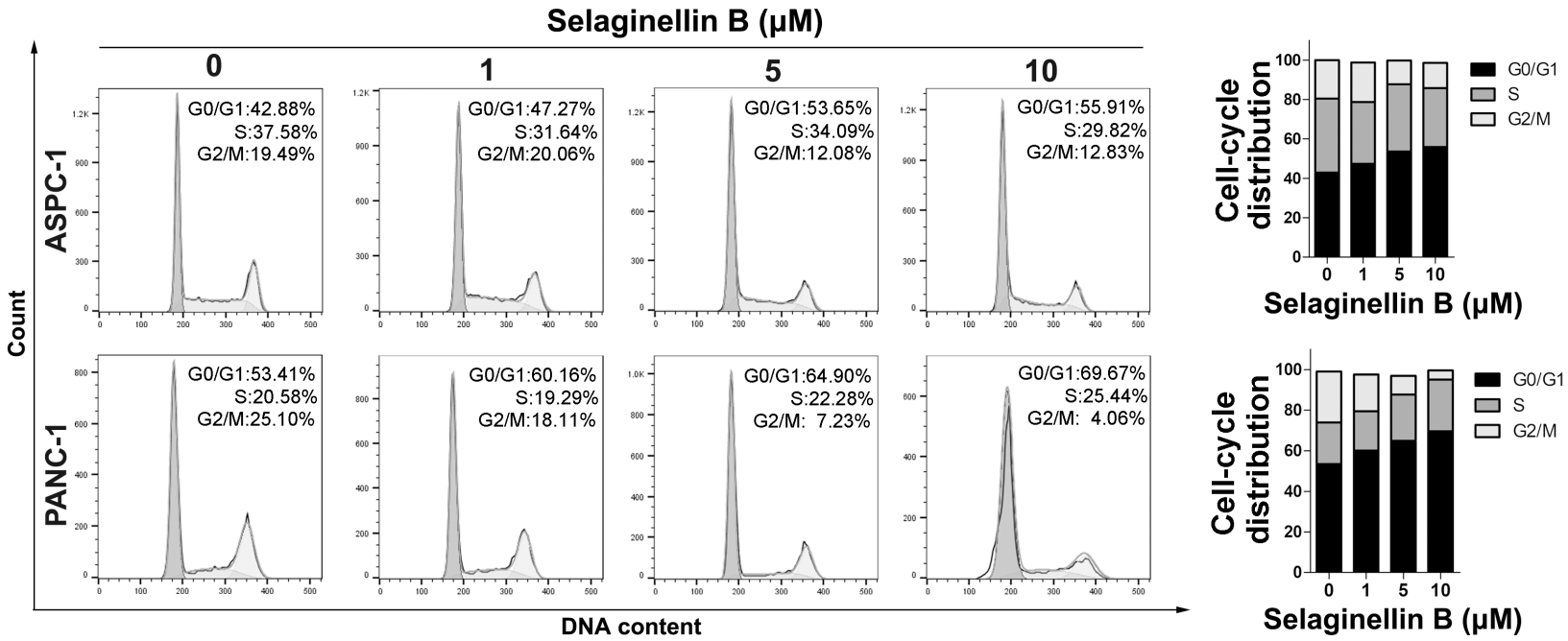

Figure 3. Analysis of the cell cycle distribution of Selaginellin B-treated ASPC-1 and PANC-1 cells. Cells were treated with different concentrations of Selaginellin B (1, 5, and 10 μM) for 24 h, and cell cycle distribution was subsequently analyzed by flow cytometry.

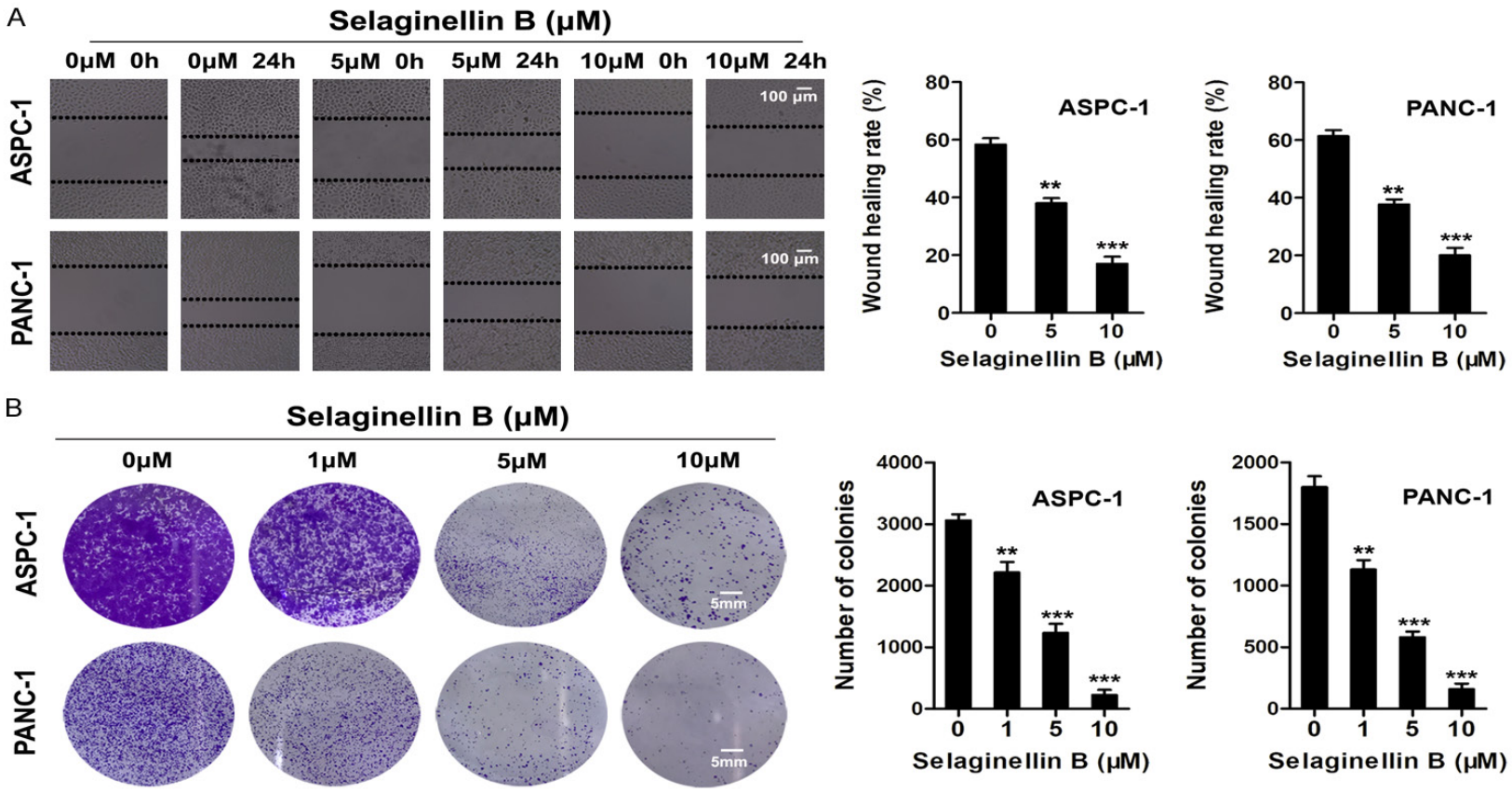

Figure 4. Selaginellin B suppressed cell migration and colony formation. A. Cell migration was analyzed by wound-healing assay. ASPC-1 and PANC-1 cells were seeded in 6-well plates, and grown until they were fully confluent. The cell migration rate was quantified. Scale bar = 100 μm. B. The ability of the ASPC-1 and PANC-1 cells to induce colony formation was also analyzed (Scale bar = 5 mm), and the colony formation rate was calculated. (All data are presented as the mean ± SD, n = 3, $^{**}P<0.01$; $^{***}P<0.001$ vs. the control group).

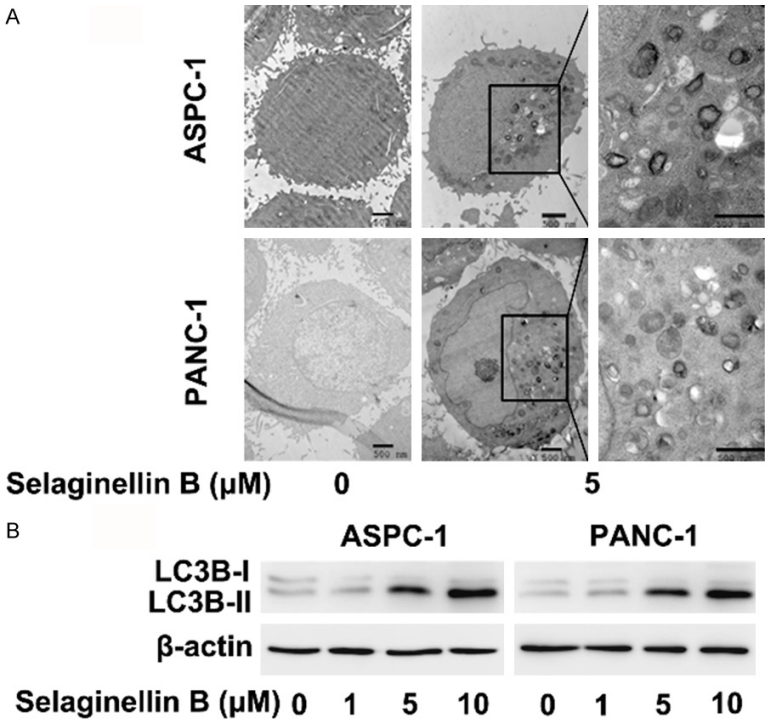

Figure 5. Induction of autophagy mediated by Selaginellin B in the ASPC-1 and PANC-1 cell lines. A. Transmission electron microscopy revealed the presence of autophagy induced by Selaginellin B in ASPC-1 and PANC-1 cells after treatment with 5 μM Selaginellin B for 24 h. B. Protein levels of the autophagy-specific marker, LC3, were detected by Western blot analysis after treatment with Selaginellin B (0, 1, 5 and 10 μM) for 24 h.

ed from migrating into the equivalent space due to their impaired migratory capability. To evaluate the influence of Selaginellin B on the clonogenic capacity of PC cells, colony formation assays were subsequently performed for the ASPC-1 and PANC-1 cell lines. **Figure 4B** showed that Selaginellin B led to a significant inhibition of colony formation, consistent with the inhibition of cell proliferation. Collectively, these results suggested that Selaginellin B was able to suppress the cell colony formation and migratory abilities of the PC cell lines.

Selaginellin B induces autophagy in PC cells

The micro-morphological changes of Selaginellin B-treated PC cells were observed by TEM, which has been demonstrated to be the most convincing method standardly employed to verify autophagy [20-22]. An intact cell and nuclear membrane architecture was observed, and the nucleus, homogeneous cytoplasm remained normal as far as the ultra-structural morphology of the untreated cells was concerned, whereas treatment with 5 μM Selaginellin B resulted in the presence of numerous vacuoles in the cytoplasm of the autophagosomes in the PC cells (**Figure 5A**). Microtubule-associated protein 1A/1B-light chain 3 (LC3), the specific marker of autophagy, was also detected by Western blot analysis (**Figure 5B**). Compared with the control group, Selaginellin B treatment increased the ratio of LC3-II/LC3-I (i.e., of the lipid-modified form to the cytosolic form). These data showed that Selaginellin B induced autophagy in both ASPC-1 and PANC-1 cells in a concentration-dependent manner. Furthermore, to provide an insight into the relationship between apoptosis and autophagy induced by Selaginellin B, the level of cleaved caspase-3 was evaluated following pre-treatment with chloroquine, an autophagy late-stage inhibitor. These results showed that pre-treatment with 10 μM chloroquine led to a marked increase in the expression of cleaved caspase-3, as compared with the group that was only treated with Selaginellin B (5 μM) (**Figure 6**). These data suggested that Selaginellin B-induced autophagy prevented cells from undergoing Selaginellin B-induced cell death, further inhibited apoptosis triggered by Selaginellin B in the ASPC-1 and PANC-1 cells.

Potential protein targets for Selaginellin B

First, potential protein target for Selaginellin B identified by virtual screening procedures with PharmMapper and the top 200 hits were sought after. Additionally, literature sources and gene database systems were consulted to decide whether the potential targets identified were associated with PC. Among the protein targets, 68 revealed a positive response. Moreover, MD simulation analysis was performed to determine the potential binding modes between Selaginellin B and the 68 protein targets. The results of the top 10 potential protein

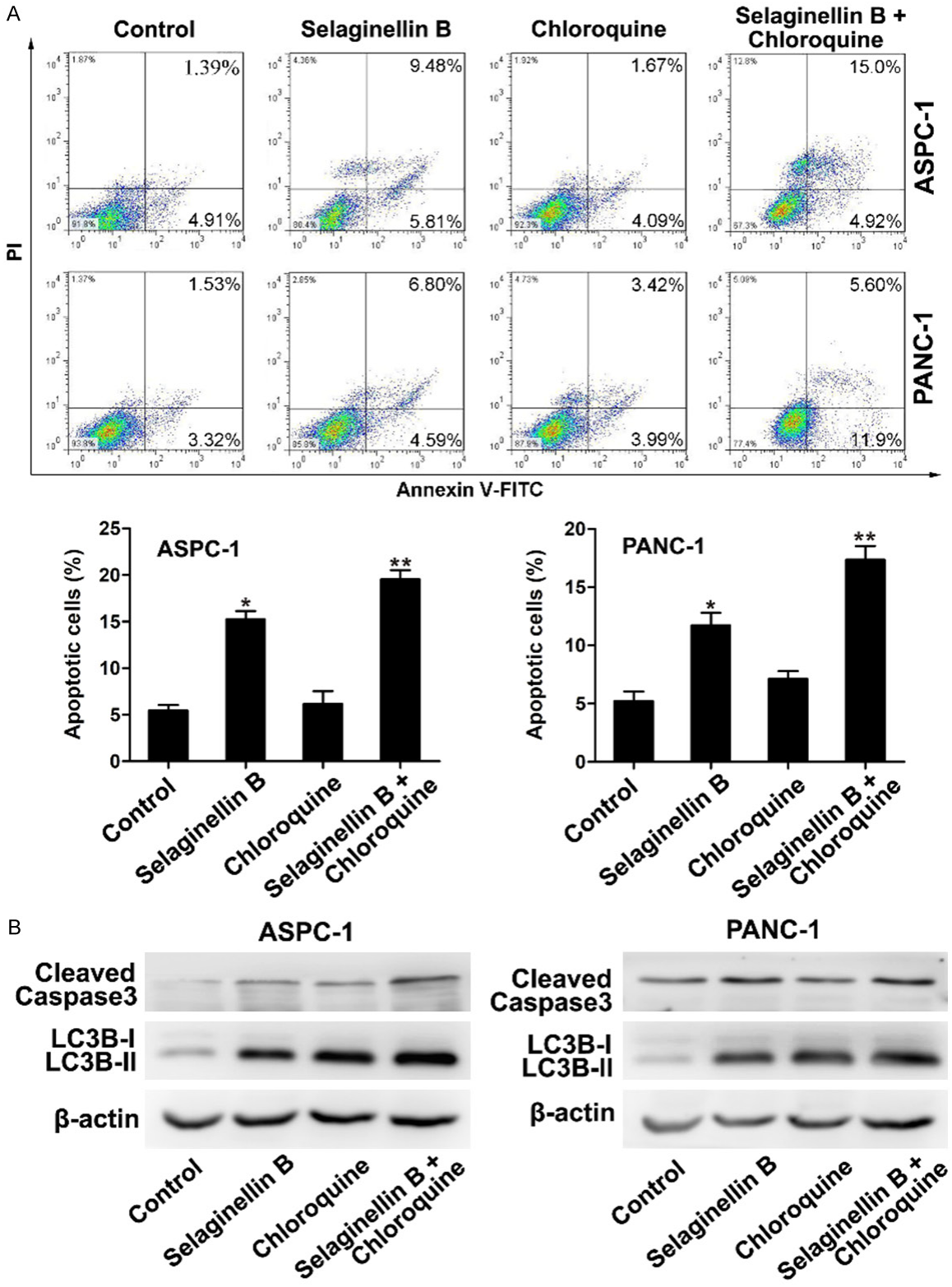

Figure 6. Effect of autophagy on the apoptosis of Selaginellin B-treated ASPC-1 and PANC-1 cells. Cells were pretreated with chloroquine (10 μM) for 2 h, and then treated with Selaginellin B (5 μM) for 24 h. A. Cell apoptosis was measured by flow cytometry. And the percentage of apoptotic cells was quantified. The dot plots have been obtained from 1 out of 3 independent experiments, performed in the same experimental conditions. Histogram data are presented as mean ± SD, n = 3. *P<0.05; **P<0.01 vs. the control group. B. Western blot analysis of LC3 and cleaved caspase-3 protein expression. Cells were pretreated with chloroquine (10 μM) for 2 h, and then treated with Selaginellin B (5 μM) for 24 h.

Table 1. Top 10 potential targets of Selaginellin B screened by PharmMapper and molecular docking

Rank	PDB ID	Name	Target Gene	Binding Affinity (kcal/mol)
2	2OJI	Mitogen-activated protein kinase 1	MAPK1	-9.4
18	2OVM	Progesterone receptor	PGR	-10.15
46	1JUJ	Thymidylate synthase	TYMS	-10.13
49	1M9R	Endothelial nitric-oxide synthase	NOS3	-11.19
52	1KBO	Nad(p)h dehydrogenase [quinone] 1	NQO1	-9.51
61	1XF0	Aldo-keto reductase family 1 member C3	AKR1C3	-11.23
76	1T4E	Ubiquitin-protein ligase e3 mdm2	MDM2	-9.97
109	1UZF	Angiotensin converting enzyme	ACE	-9.26
140	1NHZ	Glucocorticoid receptor	NR3C1	-9.73
191	2B7A	Tyrosine-protein kinase jak2	JAK2	-9.78

targets obtained from the docking simulation, and their binding affinity, are presented in **Table 1**. Lastly, the top 10 ranked potential protein targets were subjected to further MD simulation and free energy computation using the MM/PBSA methods. The results of this analysis are shown in **Figure 7A**, where the binding free energy in the JAK2 complex (-182.91 kcal/mol) was best among the top 10 of potential protein targets.

Selaginellin B inhibits JAK2 activity by targeting the ATP-binding site

STAT3 is activated through cytokines and receptor tyrosine kinases, especially JAK2. One of the integral signaling mechanisms for pancreatic carcinogenesis has been shown to involve JAK2 [14, 23]. Therefore, the effect of Selaginellin B on the protein level of JAK2 was investigated by Western blot. As shown in **Figure 7B**, Selaginellin B significantly suppressed the protein expression levels of both p-JAK2 and p-STAT3 in a concentration-dependent manner. In order to further confirm the role of Selaginellin B in regulating the JAK2/STAT3 signaling pathway in PC cells, ASPC-1 and PANC-1 cells were treated with Selaginellin B (5 μM) following pre-treatment with the JAK2 inhibitor, Fedratinib (1.5 μM) for 4 h. **Figure 7C** showed the levels of JAK2/STAT3 were significantly decreased, whereas the levels of an apoptosis-associated protein (cleaved caspase-3) were markedly increased. Furthermore, the results obtained from the docking simulation revealed what was the top-ranking docked conformation, with low binding affinity (-9.78 kcal/mol), and Selaginellin B was embedded in the active site of JAK2, fitting well within the cavity in three-dimensional space and interacting with key amino acid residues in the binding domain (**Figure 7D** and Movie S1). The fundamental interactions (highlighting the hydrogen bonds and hydrophobic interactions) are shown in **Figure 7E**, prepared using LigPlot. Specifically, in the ATP-binding site of the JAK2 kinase domain, Selaginellin B interacts with the active-site amino-acid residues (Asp939, Lys857, Asn859, and Phe860), forming four hydrogen bonds. Furthermore, Selaginellin B maintains hydrophobic interactions with the catalytic residue Asp976 and its surrounding residues, Gly861, Gly858, Asp994, Asn981, Gly993, Leu983, Gly856, Gly935, Arg980, Ser936, and Lys882, in the active site. Collectively, these results suggest that Selaginellin B inhibits JAK2 activity by targeting the ATP-binding site.

Discussion

PC is a highly lethal malignancy, and the treatment outcomes following chemotherapy at present are rather poor [24, 25]. A previous study indicated that ST exerts its anti-cancer effects against a panel of human cancers, such as breast cancer, leukemia and cervical cancer [26]. Similarly, the present study demonstrated that Selaginellin B markedly inhibits cell viability and induces cell apoptosis in ASPC-1 and PANC-1 cells. Interestingly, Selaginellin B barely exerted activities on HPDE6-C7 normal pancreatic cells, suggesting that Selaginellin B could be invoked as a protective agent in therapies against PC.

In multicellular organisms, there exists a delicate balance between the cell-generating ef-

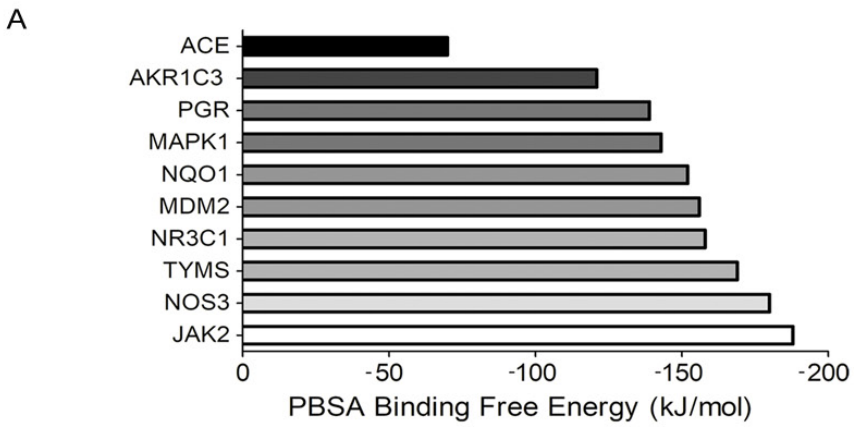
A
ACE
AKR1C3
PGR
MAPK1
NQO1
MDM2
NR3C1
TYMS
NOS3
JAK2
0
-50
-100
-150
-200
PBSA Binding Free Energy (kJ/mol)

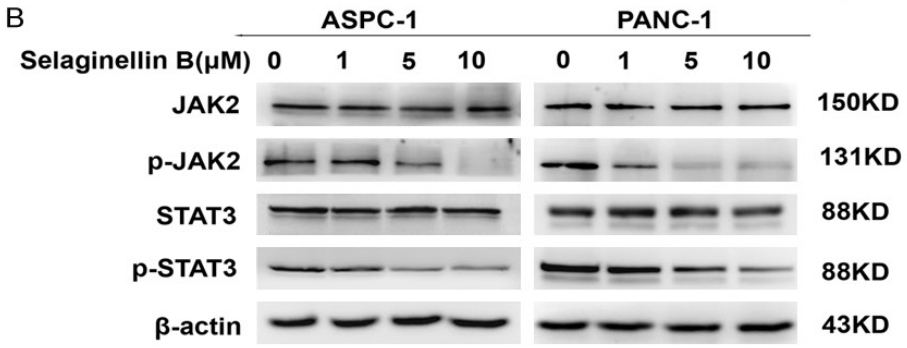
B
ASPC-1
PANC-1
Selaginellin B(μM) 0 1 5 10 0 1 5 10
JAK2
p-JAK2
STAT3
p-STAT3
β-actin
150KD
131KD
88KD
88KD
43KD

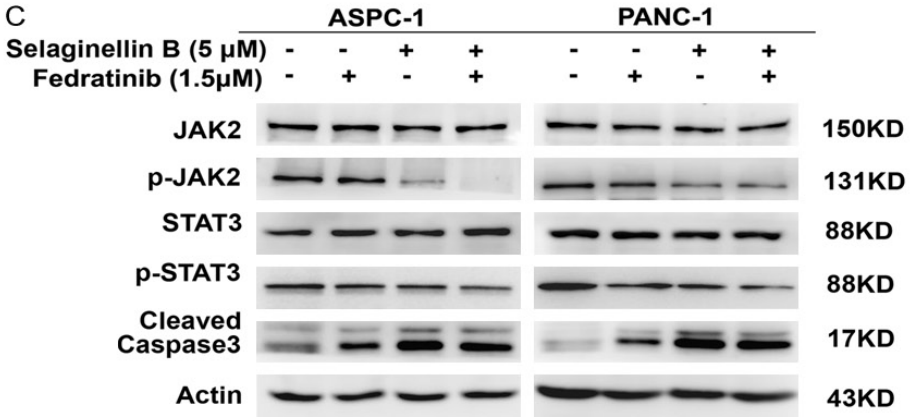
C
ASPC-1
PANC-1
Selaginellin B (5 μM) - - + + - - + +
Fedratinib (1.5μM) - + - + - + - +
JAK2
p-JAK2
STAT3
p-STAT3
Cleaved Caspase3
Actin
150KD
131KD
88KD
88KD
17KD
43KD

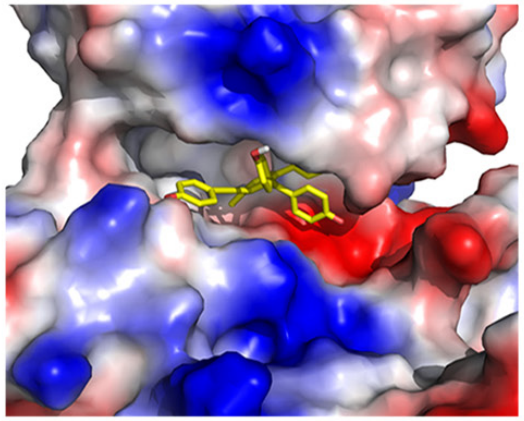
D

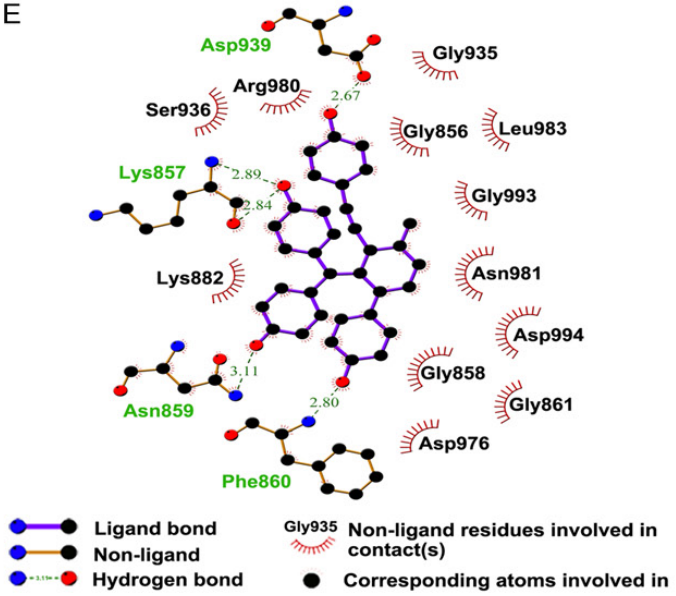
E
Asp939
Gly935
Arg980
Ser936
2.67
Gly856
Leu983
Lys857
2.89
2.84
Gly993
Lys882
Asn981
Asp994
Gly858
3.11
Asn859
Gly861
2.80
Asp976
Phe860
Ligand bond
Non-ligand
Hydrogen bond
Gly935
Non-ligand residues involved in contact(s)
Corresponding atoms involved in

Figure 7. Inhibitory effect of Selaginellin B on the JAK2/STAT3 pathway. A. The binding free energies of Selaginellin B relative to the top 10 ranked potential protein targets were calculated according to molecular dynamics simulation and MM/PBSA methods. B. ASPC-1 and PANC-1 cells were treated with Selaginellin B at the indicated doses. After 24 h of treatment, the JAK2, p-JAK2, STAT3 and p-STAT3 protein levels were analyzed by Western blotting. C. Cells were pretreated with the JAK2 inhibitor, Fedratinib (1.5 μM), for 4 h, and subsequently treated with Selaginellin B (5 μM). The protein levels of JAK2, p-JAK2, STAT3, p-STAT3 and cleaved caspase-3 were analyzed by Western blotting. D. The best ranked position of Selaginellin B (shown in yellow) in the ATP-binding site of JAK2 is presented, generated by docking. E. Two-dimensional representation of interactions of Selaginellin B in the active site of JAK2. Hydrogen bonds are displayed as green dashed lines, and the participating amino acid residues are indicated.

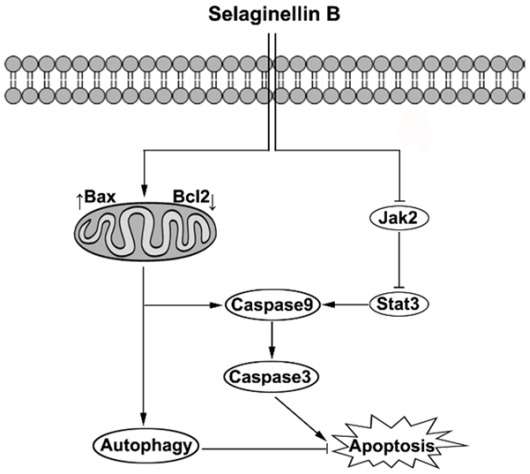

Figure 8. Selaginellin B induces autophagy and apoptosis in ASPC-1 and PANC-1 cells through activating the JAK2/STAT3 signal pathway.

fects of mitosis and apoptosis-induced cell death [27-29]. Currently, both of apoptosis and cell cycle arrest are important processes that are exploited by anticancer drugs [30, 31]. Consequently, flow cytometric analysis was performed to assess whether Selaginellin B induced cell death of the PC cells was associated with apoptosis. In this study, Selaginellin B markedly induced apoptosis in a concentration-dependent manner in the PC cells. According to the existing evidence, the receptor-mediated (extrinsic) and mitochondria-associated (intrinsic) pathways are the two major apoptotic cell death pathways [32]. ST has been shown to possess numerous pharmacological benefits, including the mediation of anti-bacterial, anti-inflammatory and anti-cancer effects [33-35]. The respective mechanisms of these pharmacological effects have been shown to be associated with the release of cytochrome *c* from the mitochondria, characterized by increases in the Bax/Bcl-2 ratio, caspase-9 and caspase-3 activity [36-38]. The action of Selaginellin B has been linked with intrinsic apoptosis, which is mediated via targeting the mitochondria.

The cell cycle, featuring its various components and stages, and cell growth and division, forms a complex biological process [39, 40]. In the present study, Selaginellin B induced anti-proliferative effects on pancreatic cells by restricting cell cycle progression, which was demonstrated through blocking G0/G1 phase in ASPC-1 and PANC-1 cells.

Several natural products have been demonstrated to exert anticancer activity, mainly via autophagy-dependent mechanisms [41-43]. Autophagy, as an evolutionarily conserved lysosomal degradation process, has an important role in regulating pro-survival and pro-death signaling pathways in numerous diseases, especially cancer. In the present study, as revealed by TEM, the autophagosomes of the ASPC-1 and PANC-1 cells upon treatment with Selaginellin B exhibited the typical appearance of containing cytoplasmic organelles and an engulfed bulk cytoplasm. Furthermore, a marked conversion of LC3I to LC3II was also detected [44, 45]. Therefore, in order to determine the association between autophagy and apoptosis induced by Selaginellin B, the extent of apoptosis in the cells, and the level of cleaved caspase-3 following pre-treatment with chloroquine, were evaluated. The findings revealed that apoptosis triggered by Selaginellin B is significantly increased following the blockade of autophagy, suggesting that autophagy induced by Selaginellin B may serve as an inhibitor of apoptosis in ASPC-1 and PANC-1 cells.

In recent years, target fishing technologies fulfill an important role in investigating the mechanism of bioactive small molecules [46, 47]. In this study, the potential protein targets of Selaginellin B were detected via reverse pharmacophore screening, molecular docking study and MD simulation. The results obtained revealed that JAK2 was the best potential protein target with the lowest PBSA binding free energy (-182.91 kcal/mol). Furthermore, the

binding model revealed that electrostatic interactions and hydrogen bonds may contribute to the binding of Selaginellin B in the ATPase catalytic site of JAK2. Therefore, Selaginellin B may possibly act as a competitive inhibitor via JAK2, and may serve as a potential antitumour drug in the future.

Several types of tumor pathogenesis have been reported due to the aberrant dysregulation of JAK/STAT signaling. In addition, JAK2/STAT3 signaling is greatly activated in PC tissues, and serves an important role in regulating cell proliferation, apoptosis, and oncogenesis in cancer cells [48-51]. However, the molecular mechanisms associated with JAK2/STAT3 signaling in apoptosis have not yet been fully explicated. The results of the present research revealed that Selaginellin B was able to suppress the expression of both p-JAK2 and p-STAT3 of ASPC-1 and PANC-1 cells in a dose-dependent manner. Compared with treatment with Selaginellin B or Fedratinib alone, treatment with both Selaginellin B and Fedratinib led to a marked increase in the levels of cleaved caspase-3, and a significant decrease in the levels of p-JAK2 and p-STAT3, indicating that the anti-proliferative effects of Selaginellin B are largely dependent on JAK2/STAT3 pathway inactivation.

In conclusion, the present study has demonstrated, for the first time, that Selaginellin B significantly decreased the cell viability of ASPC-1 and PANC-1 cells with minimal cytotoxicity in normal HPDE6-C7 cells, suggesting that Selaginellin B can selectively kill PC cells. Our results also revealed that Selaginellin B exerted its anti-tumor activity through cell cycle arrest and autophagy, which results in apoptosis via the JAK2/STAT3 signaling pathway (**Figure 8**). Therefore, Selaginellin B might provide a novel therapeutic option for the treatment of PC.

Acknowledgements

We thank the Natural Science Foundation of China (no. 81773061) and the University Innovation Team Project Foundation of Education Department of Liaoning Province (no. LT2013019).

Disclosure of conflict of interest

None.

Address correspondence to: Dr. Zhaolin Sun, Department of Biochemistry and Molecular Biology, Dalian Medical University, 9 West Section, Lvshun South Road, Dalian 116044, China. Tel: +86-131-94286901; E-mail: zlsun56@yeah.net; Dr. Zeyao Tang, Basic and Applied Research on Pharmacodynamic Substances of Traditional Chinese Medicine of Liaoning Province, 9 West Section, Lvshun South Road, Dalian Medical University, Dalian 116044, China. Tel: +86-18042662417; E-mail: tangzeyao@163.com

References

[1] Siegel RL, Miller KD and Jemal A. Cancer statistics, 2017. CA Cancer J Clin 2017; 67: 7-30.

[2] Wu X, Tang W, Marquez RT, Li K, Highfill CA, He F, Lian J, Lin J, Fuchs JR, Ji M, Li L and Xu L. Overcoming chemo/radio-resistance of pancreatic cancer by inhibiting STAT3 signaling. Oncotarget 2016; 7: 11708-23.

[3] Liu X, Wang J, Wang H, Yin G, Liu Y, Lei X and Xiang M. REG3A accelerates pancreatic cancer cell growth under IL-6-associated inflammatory condition: involvement of a REG3A-JAK2/STAT3 positive feedback loop. Cancer Lett 2015; 362: 45-60.

[4] Jiang J, Li Z, Yu C, Chen M, Tian S and Sun C. MiR-1181 inhibits stem cell-like phenotypes and suppresses SOX2 and STAT3 in human pancreatic cancer. Cancer Lett 2015; 356: 962-970.

[5] Li M, Yu X, Guo H, Sun L, Wang A, Liu Q, Wang X and Li J. Bufalin exerts antitumor effects by inducing cell cycle arrest and triggering apoptosis in pancreatic cancer cells. Tumour Biol 2014; 35: 2461-2471.

[6] Nagaraju GP, Mezina A, Shaib WL, Landry J and El-Rayes BF. Targeting the Janus-activated kinase-2-STAT3 signalling pathway in pancreatic cancer using the HSP90 inhibitor ganetespib. Eur J Cancer 2016; 52: 109-19.

[7] Neesse A, Frese KK, Chan DS, Bapiro TE, Howat WJ, Richards FM, Ellenrieder V, Jodrell DI and Tuveson DA. SPARC independent drug delivery and antitumour effects of nab-paclitaxel in genetically engineered mice. Gut 2014; 63: 974-983.

[8] Yang C, Shao Y, Li K and Xia W. Bioactive selaginellins from Selaginella tamariscina (Beauv.) spring. Beilstein J Org Chem 2012; 8: 1884-1889.

[9] Yang JS, Lin CW, Hsieh YS, Cheng HL, Lue KH, Yang SF and Lu KH. Selaginella tamariscina (Beauv.) possesses antimetastatic effects on human osteosarcoma cells by decreasing MMP-2 and MMP-9 secretions via p38 and Akt signaling pathways. Food Chem Toxicol 2013; 59: 801-807.

[10] Cheng XL, Ma SC, Yu JD, Yang SY, Xiao XY, Hu JY, Lu Y, Shaw PC, But PP and Lin RC. Selaginellin A and B, two novel natural pigments isolated from Selaginella tamariscina. Chem Pharm Bull (Tokyo) 2008; 56: 982-4.
[11] Kim JH, Cho CW, Tai BH, Yang SY, Choi GS, Kang JS and Kim YH. Soluble epoxide hydrolase inhibitory activity of selaginellin derivatives from Selaginella tamariscina. Molecules 2015; 20: 21405-21414.
[12] Chen SJ and Cui MC. Systematic understanding of the mechanism of salvianolic acid a via computational target fishing. Molecules 2017; 22: 644.
[13] Huang H, Zhang G, Zhou Y, Lin C, Chen S, Lin Y, Mai S and Huang Z. Reverse screening methods to search for the protein targets of chemopreventive compounds. Front Chem 2018; 6: 138.
[14] Zhang X, Lu H, Hong W, Liu L, Wang S, Zhou M, Chen B and Bai Y. Tyrphostin B42 attenuates trichostatin A-mediated resistance in pancreatic cancer cells by antagonizing IL-6/JAK2/STAT3 signaling. Oncol Rep 2018; 39: 1892-1900.
[15] Lu C, Talukder A, Savage NM, Singh N and Liu K. JAK-STAT-mediated chronic inflammation impairs cytotoxic T lymphocyte activation to decrease anti-PD-1 immunotherapy efficacy in pancreatic cancer. Oncoimmunology 2017; 6: e1291106.
[16] Song Y, Gao L, Tang Z, Li H, Sun B, Chu P, Qaed E, Ma X, Peng J, Wang S, Hu M and Tang Z. Anticancer effect of SZC015 on pancreatic cancer via mitochondria-dependent apoptosis and the constitutive suppression of activated nuclear factor κB and STAT3 in vitro and in vivo. J Cell Physiol 2019; 234: 777-788.
[17] Schüttelkopf AW and Van Aalten DM. PRODRG: a tool for high-throughput crystallography of protein-ligand complexes. Acta Crystallogr D Biol Crystallogr 2004; 60: 1355-1363.
[18] Trott O and Olson AJ. AutoDock Vina: improving the speed and accuracy of docking with a new scoring function, efficient optimization, and multithreading. J Comput Chem 2010; 31: 455-461.
[19] Laskowski RA and Swindells MB. LigPlot+: multiple ligand-protein interaction diagrams for drug discovery. J Chem Inf Model 2011; 51: 2778-2786.
[20] Song Y, Kong L, Sun B, Gao L, Chu P, Ahsan A, Qaed E, Lin Y, Peng J, Ma X, Zhang J, Wang S and Tang Z. Induction of autophagy by an oleanolic acid derivative, SZC017, promotes ROS-dependent apoptosis through Akt and JAK2/STAT3 signaling pathway in human lung cancer cells. Cell Biol Int 2017; 41: 1367-1378.
[21] Wang F, Xu C, Reece EA, Li X, Wu Y, Harman C, Yu J, Dong D, Wang C and Yang P. Protein kinase C-alpha suppresses autophagy and induces neural tube defects via miR-129-2 in diabetic pregnancy. Nat Commun 2017; 8: 1-14.
[22] Gao L, Wang Y, Xu Z, Li X, Wu J, Liu S, Chu P, Sun Z, Sun B, Lin Y, Peng J, Han G, Wang S and Tang Z. SZC017, a novel oleanolic acid derivative, induces apoptosis and autophagy in human breast cancer cells. Apoptosis 2015; 20: 1636-1650.
[23] Kondo R, Ishino K, Wada R, Takata H, Peng WX, Kudo M, Kure S, Kaneya Y, Taniai N, Yoshida H and Naito Z. Downregulation of protein disulfide-isomerase A3 expression inhibits cell proliferation and induces apoptosis through STAT3 signaling in hepatocellular carcinoma. Int J Oncol 2019; 54: 1409-1421.
[24] Rabi T and Catapano CV. Aphanin, a triterpenoid from Amoora rohituka inhibits K-Ras mutant activity and STAT3 in pancreatic carcinoma cells. Tumour Biol 2016; 37: 12455-12464.
[25] Biankin AV, Waddell N, Kassahn KS, Gingras MC, Muthuswamy LB, Johns AL, Miller DK, Wilson PJ, Patch AM, Wu J, Chang DK, Cowley MJ, Gardiner BB, Song S, Harliwong I, Idrisoglu S, Nourse C, Nourbakhsh E, Manning S, Wani S, Gongora M, Pajic M, Scarlett CJ, Gill AJ, Pinho AV, Rooman I, Anderson M, Holmes O, Leonard C, Taylor D, Wood S, Xu Q, Nones K, Fink JL, Christ A, Bruxner T, Cloonan N, Kolle G, Newell F, Pinese M, Mead RS, Humphris JL, Kaplan W, Jones MD, Colvin EK, Nagrial AM, Humphrey ES, Chou A, Chin VT, Chantrill LA, Mawson A, Samra JS, Kench JG, Lovell JA, Daly RJ, Merrett ND, Toon C, Epari K, Nguyen NQ, Barbour A, Zeps N; Australian Pancreatic Cancer Genome Initiative, Kakkar N, Zhao F, Wu YQ, Wang M, Muzny DM, Fisher WE, Brunicardi FC, Hodges SE, Reid JG, Drummond J, Chang K, Han Y, Lewis LR, Dinh H, Buhay CJ, Beck T, Timms L, Sam M, Begley K, Brown A, Pai D, Panchal A, Buchner N, De Borja R, Denroche RE, Yung CK, Serra S, Onetto N, Mukhopadhyay D, Tsao MS, Shaw PA, Petersen GM, Gallinger S, Hruban RH, Maitra A, Iacobuzio-Donahue CA, Schulick RD, Wolfgang CL, Morgan RA, Lawlor RT, Capelli P, Corbo V, Scardoni M, Tortora G, Tempero MA, Mann KM, Jenkins NA, Perez-Mancera PA, Adams DJ, Largaespada DA, Wessels LF, Rust AG, Stein LD, Tuveson DA, Copeland NG, Musgrove EA, Scarpa A, Eshleman JR, Hudson TJ, Sutherland RL, Wheeler DA, Pearson JV, McPherson JD, Gibbs RA and Grimmond SM. Pancreatic cancer genomes reveal aberrations in axon guidance pathway genes. Nature 2012; 491: 399-405.
[26] Jung YJ, Lee EH, Lee CG, Rhee KJ, Jung WS, Choi Y, Pan CH and Kang K. AKR1B10-inhibitory Selaginella tamariscina extract and amentoflavone decrease the growth of A549 human

lung cancer cells in vitro and in vivo. J Ethnopharmacol 2017; 202: 78-84.
[27] Prakobwong S, Gupta SC, Kim JH, Sung B, Pinlaor P, Hiraku Y, Wongkham S, Sripa B, Pinlaor S and Aggarwal BB. Curcumin suppresses proliferation and induces apoptosis in human biliary cancer cells through modulation of multiple cell signaling pathways. Carcinogenesis 2011; 32: 1372-1380.
[28] Cotter TG. Apoptosis and cancer: the genesis of a research field. Nat Rev Cancer 2009; 9: 501-507.
[29] Huang L, Hu B, Ni J, Wu J, Jiang W, Chen C, Yang L, Zeng Y, Wan R, Hu G and Wang X. Transcriptional repression of SOCS3 mediated by IL-6/STAT3 signaling via DNMT1 promotes pancreatic cancer growth and metastasis. J Exp Clin Cancer Res 2016; 35: 27.
[30] Curtin NJ. Inhibiting the DNA damage response as a therapeutic manoeuvre in cancer. Br J Pharmacol 2013; 169: 1745-1765.
[31] Gao L, Xu Z, Wang Y, Sun B, Song Z, Yang B, Liu X, Lin Y, Peng J, Han G, Wang S and Tang Z. Anticancer effect of SZC017, a novel derivative of oleanolic acid, on human gastric cancer cells. Oncol Rep 2016; 35: 1101-1108.
[32] Choudhuri T, Pal S, Das T and Sa G. Curcumin selectively induces apoptosis in deregulated cyclin D1-expressed cells at G2 phase of cell cycle in a p53-dependent manner. J Biol Chem 2005; 280: 20059-20068.
[33] Lee CW, Choi HJ, Kim HS, Kim DH, Chang IS, Moon HT, Lee SY, Oh WK and Woo ER. Biflavonoids isolated from Selaginella tamariscina regulate the expression of matrix metalloproteinase in human skin fibroblasts. Bioorg Med Chem 2008; 16: 732-738.
[34] Lee J, Choi Y, Woo ER and Lee DG. Isocryptomerin, a novel membrane-active antifungal compound from Selaginella tamariscina. Biochem Mol Biol Int 1997; 43: 489-98.
[35] Nguyen PH, Zhao BT, Ali MY, Choi JS, Rhyu DY, Min BS and Woo MH. Insulin-mimetic selaginellins from Selaginella tamariscina with protein tyrosine phosphatase 1B (PTP1B) inhibitory activity. J Nat Prod 2015; 78: 34-42.
[36] Raisova M, Hossini AM, Eberle J, Riebeling C, Wieder T, Sturm I, Daniel PT, Orfanos CE and Geilen CC. The Bax/Bcl-2 ratio determines the susceptibility of human melanoma cells to CD95/Fas-mediated apoptosis. J Invest Dermatol 2001; 117: 333-340.
[37] Chu P, Li H, Luo R, Ahsan A, Qaed E, Shopit A, Ma X, Lin Y, Peng J, Zhang J, Wang S and Tang Z. Oleanolic acid derivative SZC014 inhibit cell proliferation and induce apoptosis of human breast cancer cells in a ROS-dependent way. Neoplasma 2017; 64: 681-692.
[38] Liu H, Peng H, Ji Z, Zhao S, Zhang Y, Wu J, Fan J and Liao J. Reactive oxygen species-mediated mitochondrial dysfunction is involved in apoptosis in human nasopharyngeal carcinoma CNE cells induced by Selaginella doederleinii extract. J Ethnopharmacol 2011; 138: 184-191.
[39] Martín-Renedo J, Mauriz JL, Jorquera F, Ruiz-Andrés O, González P and González-Gallego J. Melatonin induces cell cycle arrest and apoptosis in hepatocarcinoma HepG2 cell line. J Pineal Res 2008; 45: 532-540.
[40] Tao L, Fu R, Wang X, Yao J, Zhou Y, Dai Q, Li Z, Lu N and Wang W. LL-202, a newly synthesized flavonoid, inhibits tumor growth via inducing G2/M phase arrest and cell apoptosis in MCF-7 human breast cancer cells in vitro and in vivo. Toxicol Lett 2014; 228: 1-12.
[41] Bredholt T, Dimba EA, Hagland HR, Wergeland L, Skavland J, Fossan KO, Tronstad KJ, Johannessen AC, Vintermyr OK and Gjertsen BT. Camptothecin and khat (Catha edulis Forsk.) induced distinct cell death phenotypes involving modulation of c-FLIP L, Mcl-1, procaspase-8 and mitochondrial function in acute myeloid leukemia cell lines. Mol Cancer 2009; 8: 101.
[42] Zhang DM, Liu JS, Deng LJ, Chen MF, Yiu A, Cao HH, Tian HY, Fung KP, Kurihara H, Pan JX and Ye WC. Arenobufagin, a natural bufadienolide from toad venom, induces apoptosis and autophagy in human hepatocellular carcinoma cells through inhibition of PI3K/Akt/mTOR pathway. Carcinogenesis 2013; 34: 1331-1342.
[43] Nie H, Wang Y, Qin Y and Gong XG. Oleanolic acid induces autophagic death in human gastric cancer cells in vitro and in vivo. Cell Biol Int 2016; 40: 770-778.
[44] Mizushima N, Yoshimori T and Levine B. Methods in mammalian autophagy research. Cell 2010; 140: 313-326.
[45] Baehrecke EH. Autophagy: dual roles in life and death? Nat Rev Mol Cell Biol 2005; 6: 505-510.
[46] Alvarez JV, Greulich H, Sellers WR, Meyerson M and Frank DA. Signal transducer and activator of transcription 3 is required for the oncogenic effects of non-small-cell lung cancer-associated mutations of the epidermal growth factor receptor. Cancer Res 2006; 66: 3162-3168.
[47] Giordano C, Vizza D, Panza S, Barone I, Bonofiglio D, Lanzino M, Sisci D, De Amicis F, Fuqua SA, Catalano S and Andò S. Leptin increases HER2 protein levels through a STAT3-mediated up-regulation of Hsp90 in breast cancer cells. Mol Oncol 2013; 7: 379-391.
[48] Huang L, Huang Z, Lin W, Wang L, Zhu X, Chen X, Yang S and Lv C. Salidroside suppresses the

growth and invasion of human osteosarcoma cell lines MG63 and U2OS in vitro by inhibiting the JAK2/STAT3 signaling pathway. Int J Oncol 2019; 54: 1969-1980.

[49] Zhang Z, Wang F, Du C, Guo H, Ma L, Liu X, Kornmann M, Tian X and Yang Y. BRM/SMARCA2 promotes the proliferation and chemoresistance of pancreatic cancer cells by targeting JAK2/STAT3 signaling. Cancer Lett 2017; 402: 213-224.

[50] Zhong HJ, Lin S, Tam IL, Lu L, Chan DS, Ma DL and Leung CH. In silico identification of natural product inhibitors of JAK2. Methods 2015; 71: 21-25.

[51] Gallmeier E, Schäfer C, Moubarak P, Tietz A, Plössl I, Huss R, Göke B and Wagner AC. JAK and STAT proteins are expressed and activated by IFN-gamma in rat pancreatic acinar cells. J Cell Physiol 2005; 203: 209-216.

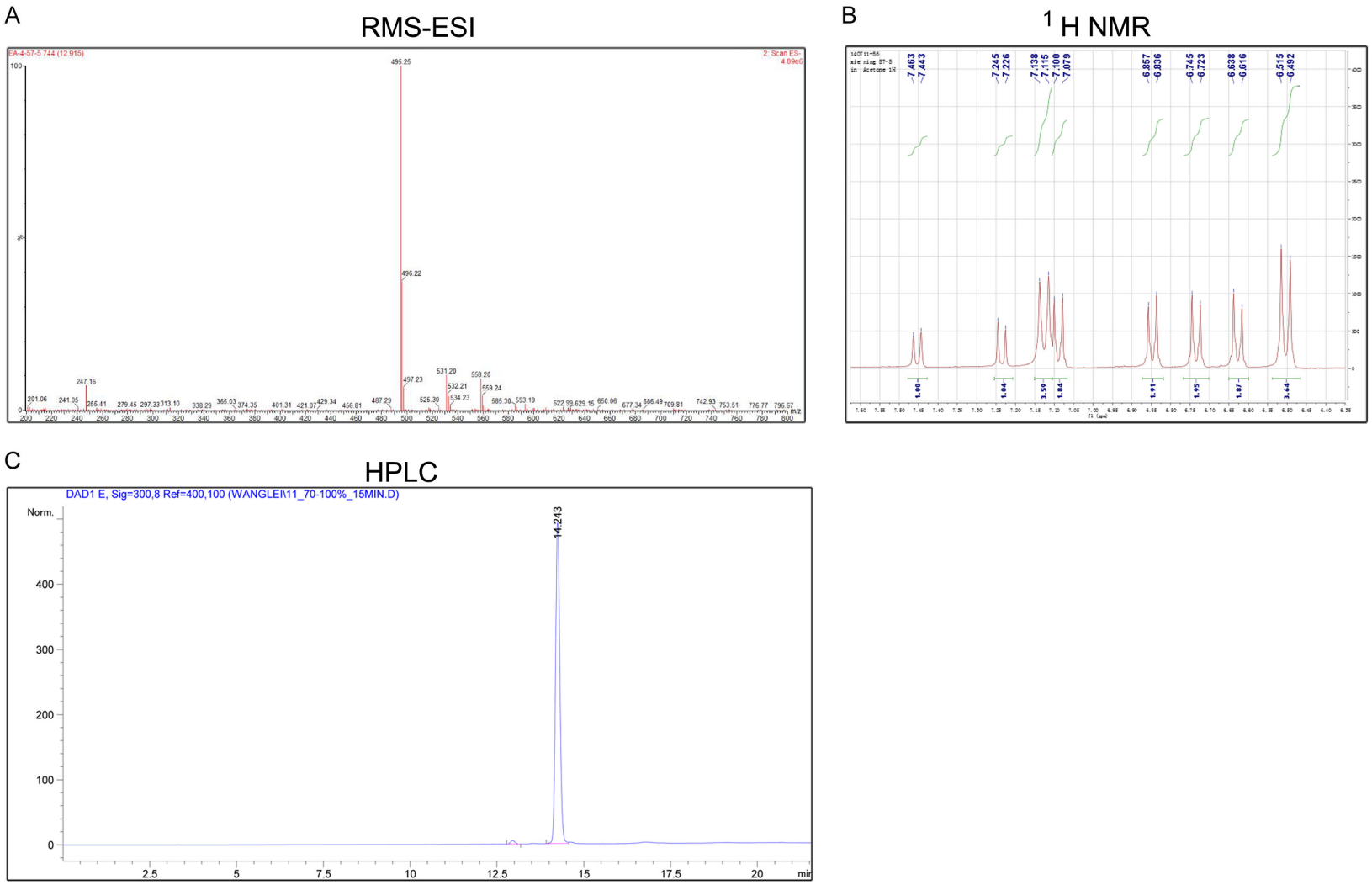

Figure S1. The purity of Selaginellin B was confirmed by ESI-MS, ^{1}H-NMR and HPLC analyses. A. ESI-MS results, showing the molecular mass of Selaginellin B. B. Proton NMR (^{1}H-NMR) analysis, revealing the exact integration and positions of the protons pertaining to Selaginellin B. C. HPLC profile of Selaginellin B, revealing the purity to be 98.7%.

Movie S1. Movie of 20 ns of MD simulation of Selaginellin B complexed in the pocket of JAK2. JAK2 is shown in cyan, whereas Selaginellin B is shown in the orange sphere model. MD, molecular dynamics; JAK2, Janus kinase 2.